Available online at www.elixirpublishers.com (Elixir International Journal)

Vibrational Spectroscopy

Elixir Vib. Spec. 86 (2015) 35018-35027

ISSN: 2229-712X

Vibrational Spectral Study of 2,4,4 -trimethyl-2-oxazoline with Density Functional Theory, NBO and HOMO-LUMO Analyses

M. Elanthiraiyan[1], B. Jayasudha[2,*], M. Arivazhagan[3] and N.Saravanan[4]

[1]Department of Physics, National College, Tiruchirappalli 620001, India.
[2]Department of Physics, H. H. The Rajah's College, Pudukkottai 622001, India.
[3]Department of Physics, Govt.Arts College, Tiruverumbur, Tiruchirappalli 620022, India.
[4]Department of Chemistry, A.A.Government Arts College, Musiri-621211. Trichy, Tamilnadu, India.

ARTICLE INFO

Article history:
Received: 14 July 2015;
Received in revised form:
31 August 2015;
Accepted: 9 September 2015;

Keywords
2,4,4-Trimethyl-2-oxazoline,
FT-IR,
FT- Raman,
HOMO-LUMO,
DFT.

ABSTRACT

The FT-IR and FT Raman spectra of 2,4,4-Trimethyl-2-oxazoline (TMOZ) molecule have been recorded in the region 4000-400cm^{-1} and 3500-50cm^{-1} respectively. Optimized geometrical parameters, harmonic vibrational frequencies and depolarization ratio have been computed by density functional theory (DFT) using B3LYP/6-31+G(d,p) and B3LYP/6-311++G(d,p) method and basis sets. The observed FT-IR and FT-Raman vibrational frequencies are analysed and compared with theoretically predicted vibrational frequencies. The geometries and normal modes of vibration obtained from DFT method are in good agreement with the experimental data. The Mulliken charges, the natural bonding orbital (NBO) analysis, the values of electric dipole moment (μ) and the first-order hyperpolarizability (β_0) of the investigated molecule were computed using DFT calculations. The calculated HOMO and LUMO energies shows that charge transfer occur within molecule. The influences of oxygen and hydrogen atoms on the geometry of benzene and its normal modes of vibrations have also been discussed. Unambiguous vibrational assignments of all the fundamentals was made using the total energy distribution (TED).

Introduction

Oxazoline is a five-membered heterocyclic organic compound containing one atom of oxygen and nitrogen. It exists between oxazole and oxazolidine in terms of saturation. Compounds containing this ring are referred to as oxazolines or oxazolyls and have a variety of chemical uses; particularly as ligands in asymmetric catalysis and as protecting groups for carboxylic acids. Owing to study of oxazolines compounds is considerable importance of 2,4,4-Trimethyl-2-oxazoline (TMOZ) the vibrational frequencies are determined using quantum chemical calculations. The assignments of band in the vibrational spectra of the molecules are an essential step in the application of vibrational spectroscopy for solving various structural chemical problems. The literature survey reveals that no theoretical calculations or detailed vibrational infrared and Raman analysis have been performed on 2,4,4-Trimethyl-2-oxazoline (TMOZ) so far. Hence, in the present investigation, the geometrical parameters and vibrational wave numbers of TMOZ are investigated by using *ab initio* HF and B3LYP calculations with 6-311++G(d,p) basis set. Specific scale factors are also used and employed in the predicted frequencies.

The computed values of the polarizability (α_0) and the first hyperpolarizability (β) of the investigated molecule computed show that the TMOZ molecule might have microscopic nonlinear optical (NLO) behaviour with non-zero values. The thermodynamic properties, Mulliken charges, Natural Bond Orbitals (NBO) and molecular electro static potential (MEP) are also analyzed.

Experimental Details

The pure sample of TMOZ is obtained from Lancaster chemical company, UK and used as such without any further purification to record FT-IR and FT-Raman spectra. The room temperature Fourier transform IR spectrum of TMOZ is measured in the 4000 - 400 cm^{-1} region at a resolution of ± cm^{-1} using BRUKER IFS-66V Fourier transform spectrometer equipped with an MCT detector, a KBr beam splitter and globar arc source.

The FT-Raman spectrum is recorded on a BRUKER IFS-66V model interferometer equipped with an FRA-106 FT-Raman accessory. The FT-Raman spectrum is recorded in the 3500 – 50 cm^{-1} stokes region using the 1064 nm line of Nd:YAG laser for the excitation operation at 200mW power. The reported wave numbers are expected to be accurate within ± 1 cm^{-1}.

Prediction of Raman Intensities

The Raman activities (S_i) calculated with the GAUSSIAN 09W program are subsequently converted to relative Raman intensities (I_i) using the following relationship derived from the basic theory of Raman scattering, [1-3]

$$I_i = \frac{f(\nu_0 - \nu_i)^4 S_i}{\nu_i \left[1 - \exp\left(-\frac{hc\nu_i}{K_b T}\right)\right]}$$

where ν_0 is the exciting frequency in cm^{-1}, ν_i the vibrational wave number of the ith normal mode, h, c and k_b are the fundamental constants and f is a suitably chosen common normalization factor for all the peak intensities.

Computational Methods

The molecular structure of TMOZ in the ground state is computed using HF and B3LYP with 6-311++G (d,p) basis set. All the computations have been done by adding polarization function and diffuse function on heavy atoms [4,5], in addition to triple split valence basis set 6-311++G(d,p), for better treatment of polar bonds of methoxy group. The theoretical results have enabled us to make the detailed assignments of the experimental IR and Raman spectra of the title compound. The

---

Tele:
E-mail addresses: jjmarivu@yahoo.co.in

DFT and HF calculations for TMOZ are performed using GAUSSIAN 09W program without any constraint on the geometry [6].

Results and Discussion

Geometry optimization

The molecular structure along with the numbering of atoms of TMOZ is obtained from Gaussian 09W and GAUSSVIEW programmes and shown in Fig.1.

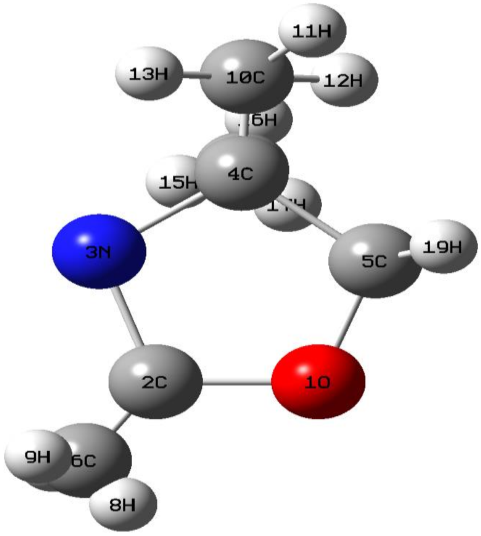

Fig 1. The optimized structure of 2,4,4-trimethyl-2-oxazoline

The global minimum energy obtained by HF and DFT/B3LYP structure optimization using with 6-311++G(d,p) basis sets for the title molecule are -362.9351a.u. and -365.1402a.u. respectively. The most optimized structural parameters calculated by HF and DFT/B3LYP levels with 6-311++G(d,p) basis sets are presented in Table 1. Detailed description of vibrational modes can be given by means of normal co-ordinate analysis. For this purpose, the full set of 51 standard internal co-ordinates (containing 14 redundancies) for the title compound is presented in the Table 2. From these, a non redundant set of local symmetry co-ordinates were constructed by suitable linear combinations of internal co-ordinates following the recommendations of Pulay et al. (X, Y) which are presented in Table 3.

Vibrational analysis

The vibrational spectral analysis of TMOZ is based on FT-IRand Raman pectra. (Figs. 2 and 3)

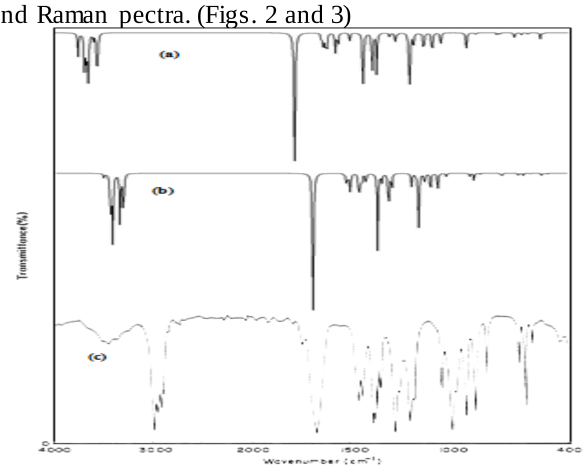

Fig 2. Comparison of observed and calculated FT-IR spectra of 2,4,4-trimethyl-2- oxazoline (a) observed, (b) calculated with B3LYP/6-311++G(d,p) and (c) calculated with HF/6-311++G(d,p)

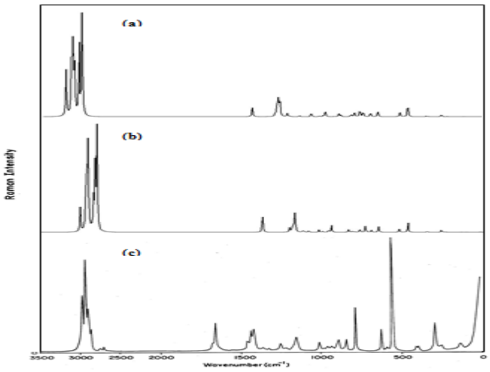

Fig 3. Comparison of observed and calculated FT-Raman spectra of 2,4,4-trimethyl-2- oxazoline (a) observed (b) calculated with B3LYP/6-311++G(d,p) and (c) calculated with HF/6-311++G(d,p)

The TMOZ consists of 19 atoms, which has 51 normal modes. The 51 normal modes of TMOZ have been assigned according to the detailed motion of the individual atoms. This compound belongs to C_1 point group symmetry. The computed vibrational wavenumbers and the atomic displacements corresponding to the different normal modes are used for identifying the vibrational modes unambiguously. The calculated vibrational wavenumbers, measured infrared and Raman band positions and their assignments are given in Table 4. Total energy distribution (TED) is calculated by using the scaled quantum mechanical program (SQM) and fundamental vibrational modes are characterized by their TED.

Methyl group vibrations

For the assignments of CH_3 group frequencies, nine fundamentals can be associated to each CH_3 group namely, CH_3 symmetrical stretch, CH_3 in-plane stretch (i.e., in-plane hydrogen stretching modes), CH_3 in-plane bending (i.e., hydrogen deformation modes), CH_3 symmetrical bending, CH_3 in-plane rocking, CH_3 out-of-plane rocking and CH_3 twisting. In addition to that, CH_3 out-of-plane stretch and CH_3 out-of-plane bending modes of the CH_3 group would be expected to be depolarized for a symmetry species. The C–H stretching in CH_3 occurs at lower frequencies than those of aromatic ring (2925–3000 cm^{-1}). The vibrations of methyl group in this title molecule are observed in the typical range reported earlier [7-10]. The CH_3 symmetric stretching frequencies are established at 2965, 2960 and 2953 cm^{-1} whereas CH_3 asymmetric frequencies are assigned at 2936 and 2903 cm^{-1} in FT Raman and 2982 cm^{-1} in FT-IR spectrum. The asymmetric deformation of CH_3 group is usually observed at around 1450cm^{-1} for methyl substituted aromatic rings [11, 12]. As predicted in the literature [11, 12] bands appeared in this title compound at 1458 and 1445 cm^{-1} in FT Raman spectrum and 1436 cm^{-1} in FTIR are assigned to CH_3 in-plane bending deformation vibrations. The peaks at 1369 1352 and 1346 cm^{-1} are assigned to CH_3 out of plane bending deformation vibrations. The peaks at 1276 cm^{-1} and 1201 cm^{-1} in FTIR spectrum and the peak observed at 1179 cm^{-1} in FT – Raman cm^{-1} spectrum are assigned to CH_3 in-plane rocking modes. The bands observed at 1049, 1038 and 992 cm^{-1} are assigned to CH_3 out-of-plane rocking modes while the frequencies at 340, 300 and 180 cm^{-1} are assigned to CH_3 torsion mode are shown in the Table 4.

C–C vibrations

C–C stretching vibrations usually occur in 1400-1625 cm^{-1} region [13,14]. In present study the bands for C-C stretching vibrations are observed at1689, 1679, 1674 and 1666 cm^{-1}[15]. The C–C stretching frequencies have deviated little due to the conjugated effect and CH_2, CH_3 substitutions. The peaks at 885, 874, 822 and 680, 665, 655 cm^{-1} are assigned to C–C in-plane-bending vibrations and out-of-plane bending vibrations respectively. These assignments are in good agreement with the literature [16-18].

C-O vibrations

The carbonyl group vibrational frequencies are the significant characteristic bands in the vibrational spectra of ketones, and for this reason, such bands have been the subject of extensive studies [19-22]. The intensity of these bands can increase because of conjugation, therefore, leads to the intensification of the Raman lines as well as the increased infrared band intensities. In the present investigation, the FTIR band of TMOZ observed at 1490, 1465 cm^{-1} is assigned as C-O stretching vibration.

C-N Vibrations

In heterocylic compounds, the C-N stretching vibration usually occurs in the region 1400-1200 cm^{-1}. Mixing of vibrations are possible in this region so identification of C-N stretching is little bit a difficult task [23-26]. In this study, the bands observed at 1781 and 1739 cm^{-1} in FTIR have been assigned to C-N stretching vibration of TMOZ. These assignments are also supported by the TED values.

CH_2 Group Vibrations

There are six fundamentals that can be associated to each CH_2 group namely CH_2 symmetric stretching, CH_2 asymmetric stretching, CH_2 scissoring and CH_2 rocking which belongs to in-plane vibrations and two out-of-plane vibrations, viz., CH_2 wagging and CH_2 twisting modes, which are expected to be depolarized [27]. The asymmetric CH_2 stretching vibrations are generally observed above 3000 cm^{-1}, while symmetric stretching will appear between 3000 and 2900 cm^{-1} [28-30]. CH_2 symmetric and asymmetric vibrations are observed at 2727 and 2713 cm^{-1} in FT – IR spectrum for TOMZ. For TOMZ the CH_2 scissoring vibrations observed at 1409 cm^{-1} in FT-IR spectrum. The band at 463 cm^{-1} is assigned to CH_2 rocking vibration [31]. The CH_2 wagging and twisting vibrations observed at 918 cm^{-1} and 811 cm^{-1} of TMOZ respectively, are exactly coincides with the reported value of the early work [32].

Non-linear Optical Effects

Polarizabilities and hyperpolarizabilities characterize the response of a system in an applied electric field [33]. They determine not only the strength of molecular interactions (long-range intermolecular induction, dispersion forces, etc.) as well as the cross sections of different scattering and collision processes, but also the non-linear optical properties (NLO) of the system [34, 35]. It has been found that the dye sensitizer hemicyanine system, which has high NLO property, usually possesses high photoelectric conversion performance [36]. The polarizabilities and hyperpolarizabilities are used to investigate the relationships among photocurrent generation, molecular structures and NLO [37].

The first hyperpolarizability (β) of the molecular system, and related properties (α_0 and Δα) of TMOZ are calculated using B3LYP/6-311++G (d,p) basis set, based on the finite-field approach. In the presence of an applied electric field, the energy of a system is a function of the electric field. First hyperpolarizability is a third rank tensor that can be described by a 3 × 3 × 3 matrix. The 27 components of the 3D matrix can be reduced to 10 components due to the Kleinman symmetry [38]. It can be given in the lower tetrahedral format. It is obvious that the lower part of the 3 × 3 × 3 matrix is a tetrahedral. The components of β are defined as the coefficients in the Taylor series expansion of the energy in the external electric field. When the external electric field is weak and homogeneous, this expansion becomes:

$$E = E^0 - \mu_\alpha F_\alpha - \frac{1}{2}\alpha_{\alpha\beta}F_\alpha F_\beta - \frac{1}{6}\beta_{\alpha\beta\gamma} F_\alpha F_\beta F_\gamma + \ldots$$

Where E^0 is the energy of the unperturbed molecules, F_α, the field at the origin and μ_α, $\alpha_{\alpha\beta}$ and $\beta_{\alpha\beta\gamma}$ are the components ofdipole moment, polarizability and the hyperpolarizability, respectively. The total static dipole moment μ, the mean polarizability α_0, the anisotropy of the polarizability Δα and the mean first hyperpolarizability β, using the X, Y, Z components they are defined as follows:

$\mu = (\mu^2_x+\mu^2_y+\mu^2_z)^{1/2}$

$\alpha_0 = (\alpha_{xx}+\alpha_{yy}+\alpha_{zz})/3$

$\beta = (\beta^2_x+\beta^2_y+\beta^2_z)^{1/2}$ and

$\beta_x = \beta_{xxx} + \beta_{xyy} + \beta_{xzz}$

$\beta_y = \beta_{yyy} + \beta_{xxy} + \beta_{yzz}$

$\beta_z = \beta_{zzz} + \beta_{xxz} + \beta_{yyz}$

Since the standard values of the polarizability α and first hyperpolarizability β are reported in atomic units (a.u.), the calculated values should have been converted into electrostatic units (esu). (α: 1 a.u. = 0.1482 × 10^{-24} e.s.u; β: 1 a.u. = 8.6393 × 10^{-33} e.s.u) [39]. The calculated total static dipole moment (μ), mean polarizability (α_0) and hyperpolarizability (β) are 1.45534 Debye, 13.6969 × 10^{-24} e.s.u and 6.7438 × 10^{-30} e.s.u by DFT method.

Thermodynamic Properties

The thermodynamic parameters such as total thermal energy, heat capacity at constant volume, entropy, vibrational energy, zero point vibrational energy and rotational constants are calculated employing HF/6-311++G(d,p) and B3LYP/6-311++G(d,p) methods and they are presented in Table 5. Dipole moment reflects the molecular charge distribution and is given as a vector in three dimensions. Therefore, it can be used as descriptor to depict the charge movement across the molecule. Direction of the dipole moment vector in a molecule depends on the centers of positive and negative charges. Dipole moments are strictly determined for neutral molecules. For charged systems, its value depends on the choice of origin and molecular orientation.

Mulliken's Atomic Charge

The bonding capability of a molecule depends on the electronic charge on the chelating atoms. The atomic charge values are obtained by the Mulliken population analysis [40]. To validate the reliability of the results, the Mulliken population analysis of TMOZ is calculated using HF and B3LYP levels of theory with 6-311++G(d,p) basis set. The corresponding characteristics of the atomic charge populations of the constituent atoms and bonds are presented in Table 6. In TMOZ molecule the charge on C1, C2 and C3 atoms are negative whereas the remaining carbons, sulphur and hydrogen atoms are positively charged. The result suggests that the atoms bonded to the hydrogen atom and the oxygen atoms are electron acceptor. The graphical representation of Mulliken population of TMOZ is shown in Fig 4. The maximum charge is obtained for carbonyl carbon (C2) when compared with all other atoms.

Natural Bond Orbital (NBO) Analysis

It has become well known that among theoretical methods, natural bond orbital (NBO) analysis developed by Weinhold *et. al.,* [41-43] is an extraordinary useful formalism to evaluate delocalization effects.

Table 1. Optimized geometrical parameters of 2,4,4-trimetlyl-2-oxazoline obtained by HF/6-311++G(d,p) and B3LYP/6 311++G(d,p) methods and basis set

Bond Length	Value (Å)		Bond Angle	Value (°)		Dihedral Angle	Value (°)	
	6-311++G(d,p)			6-311++G(d,p)			6-311++G(d,p)	
	HF	B3LYP		HF	B3LYP		HF	B3LYP
O1-C2	1.3449	1.3712	C2-O1-C5	106.9754	106.038	C5-O1-C2-N3	0.028	0.015
O1-C5	1.4223	1.4489	O1-C2-N3	117.9477	118.213	C5-O1-C2-C6	180.030	180.014
C2-N3	1.2515	1.2741	O1-C2-C6	115.114	114.842	C2-O1-C5-C4	-0.041	-0.027
C2-C6	1.4908	1.4921	N3-C2-C6	126.9382	126.944	C2-O1-C5-H18	120.885	120.951
N3-C4	1.4651	1.4814	C2-N3-C4	108.1218	107.772	C2-O1-C5-H19	-120.974	-121.010
C4-C5	1.5525	1.5622	N3-C4-C5	102.896	103.397	O1-C2-N3-C4	0.000	0.005
C4-C10	1.5292	1.5357	N3-C4-C10	109.5019	109.258	C6-C2-N3-C4	179.998	180.006
C4-C14	1.5292	1.5357	N3-C4-C14	109.4985	109.262	O1-C2-C6-H7	-59.115	-59.221
C5-H18	1.082	1.0943	C5-C4-C10	112.1097	111.998	O1-C2-C6-H8	59.261	59.224
C5-H19	1.082	1.0943	C5-C4-C14	112.1072	111.999	O1-C2-C6-H9	-179.930	-180.002
C6-H7	1.0845	1.0949	C10-C4-C14	110.4432	110.638	N3-C2-C6-H7	120.881	120.777
C6-H8	1.0845	1.0949	O1-C5-C4	104.059	104.578	N3-C2-C6-H8	-120.735	-120.776
C6-H9	1.0801	1.0901	O1-C5-H18	108.2865	107.979	N3-C2-C6-H9	0.071	0.001
C10-H11	1.0853	1.0941	O1-C5-H19	108.2864	107.980	C2-N3-C4-C5	-0.026	-0.022
C10-H12	1.0842	1.0965	C4-C5-H18	113.4006	113.336	C2-N3-C4-C10	119.360	119.39
C10-H13	1.0872	1.0949	C4-C5-H19	113.4056	113.339	C2-N3-C4-C14	-119.409	-119.437
C14-H15	1.0872	1.0965	H18-C5-H19	109.071	109.268	N3-C4-C5-O1	0.0411	0.031
C14-H16	1.0842	1.0941	C2-C6-H7	109.8814	110.215	N3-C4-C5-H18	-117.398	-117.328
C14-H17	1.0853	1.0949	C2-C6-H8	109.8784	110.216	N3-C4-C5-H19	117.483	117.391
			C2-C6-H9	109.8147	109.651	C10-C4-C5-O1	-117.518	-117.480
			H7-C6-H8	107.7798	107.459	C10-C4-C5-H18	125.041	125.160
			H7-C6-H9	109.7511	109.633	C10-C4-C5-H19	-0.076	-0.119
			C4-C10-H11	110.8294	110.221	C14-C4-C5-O1	117.595	117.545
			C4-C10-H12	110.228	110.781	C14-C4-C5-H18	0.155	0.186
			C4-C10-H13	110.0119	108.489	C14-C4-C5-H19	-124.962	-125.094
			H11-C10-H12	108.0119	108.489	N3-C4-C10-H11	-58.427	-59.021
			H11-C10-H13	108.3387	108.056	N3-C4-C10-H12	61.095	60.941
			H12-C10-H13	108.4135	108.411	N3-C4-C10-H13	-178.818	-178.102
			C4-C14-H15	110.9272	110.782	C5-C4-C10-H11	55.112	56.113
			C4-C14-H16	110.2288	110.222	C5-C4-C10-H12	174.638	174.638
			C4-C14-H17	110.8262	110.799	C5-C4-C10-H13	-65.275	-65.275
			H15-C14-H16	108.4134	108.487	C14-C4-C10-H11	-179.085	-178.085
			H15-C14-H17	108.3398	108.410	C14-C4-C10-H12	-59.562	-59.862
			H16-C14-H17	108.0124	108.056	C14-C4-C10-H13	60.524	60.824
						N3-C4-C14-H15	178.794	179.190
						N3-C4-C14-H16	-61.117	-60.728
						N3-C4-C14-H17	58.504	58.826
						C5-C4-C14-H15	65.255	65.243
						C5-C4-C14-H16	-174.565	-174.674
						C5-C4-C14-H17	-55.134	-55.122
						C10-C4-C14-H15	-60.545	-60.480
						C10-C4-C14-H16	59.542	59.599
						C10-C4-C14-H17	179.064	179.155

Table 2. Definition of internal coordinates of 2, 4, 4-trimetlyl-2-oxazoline

No (i)	Symbol	Type	Definition[a]
Stretching			
1 – 3	r_i	C-H$_3$ methyl	($C_6 – H_7$), ($C_6 – H_8$), $C_6 – H_9$
4 – 6	r_i	C-H$_3$	$C_{10} – H_{11}$, $C_{10} – H_{12}$, $C_{10} – H_{13}$
7 – 9	r_i	C-H$_3$	$C_{14} – H_{15}$, $C_{14} – H_{16}$, $C_{14} – H_{17}$
10-11	Υ_i	C-H$_2$	$C_5 – H_{18}$, $C_5 – H_{19}$
12-15	s_i	C-C	$C_2 – C_6$, $C_4 – C_{10}$, $C_4 – C_{14}$, $C_4 – C_5$
16-17	R_i	C-O	$C_5 – O_1$, $C_2 – O_1$
18-19	T_i	C-N	$C_4 – N_3$, $C_2 – N_3$

In-plane bending			
20 -24	π_i	bend	$O_1 – C_2 – N_3$, $C_2 – N_3 – C_4$, N_3-C_4-C_5, C_4-C_5-O_1, C_5-O_1-C_2
25– 33	λ_i	C-C-H	$C_2 – C_6 – H_9$, $C_2 – C_6 – H_8$, $C_2 – C_6 – H_7$, $C_4 – C_{10} – H_{11}$, $C_4 – C_{10} – H_{12}$, $C_4 – C_{10} – H_{13}$, $C_4 – C_{14} – H_{15}$, $C_4 – C_{14} – H_{16}$, $C_4 – C_{14} – H_{17}$
34 -42	σ_i	H-C-H	$H_8 – C_6 – H_3$, $H_8 – C_6 – H_2$, $H_7 – C_6 – H_9$ $H_{11} – C_{10} – H_{12}$, $H_{12} – C_{10} – H_{13}$, $H_{11} – C_{10} – H_{13}$ $H_{15} – C_{14} – H_{16}$, $H_{15} – C_{14} – H_{17}$, $H_{16} – C_{14} – H_{17}$
43-44	β_i	C-C-H	$C_4 – C_5 – H_{18}$, $C_4 – C_5 – H_{19}$
45-46	β_i	O-C-H	$O_1 – C_5 – H_{18}$, $O_1 – C_5 – H_{19}$
47	ϕ_i	N-C-C	$N_3 – C_2 – C_6$
48	θ_i	O-C-C	$O_1 – C_2 – C_6$
49-50	ξ_i	N-C-C	$N_3 – C_4 – C_{10}$, N_3 - C_4 - C_{14}
51-52	ξ_i	C-C-C	C_5- C_4-C_{10}, C_5 - C_4 - C_{14},
Out-of-plane bending			
53-55	ω_i	C-C	C_6-C_2-N_3-O_1, C_{10}-C_4-N_3-C_5, C_{14}-C_4-N_3-C_5
Torsion			
56-60	τ_i	τ bend	$O_1 – C_2 – N_3 – C_4$, $C_2 – N_3 – C_4 – C_5$, $N_3 – C_4 – C_5 – O_1$, $C_4 – C_5 – O_1 – C_2$, $C_5 – O_1 – C_2 – N_3$
61	τ_i	$\tau C–CH_3$	$(O_1,N_3) – C_2 – C_6$-(H_7, H_8, H_9)
62	τ_i	$\tau C–CH_3$	(N_3,C_5)- $C_4 – C_{10} – (H_{11}, H_{12}, H_{13})$
63	τ_i	$\tau C–CH_3$	(N_3,C_5)- $C_4 – C_{14} – (H_{15}, H_{16}, H_{17})$

[a] For numbering of atoms refer Fig.1.

Table 3. Definition of local symmetry coordinates of 2,4,4-trimetlyl-2-oxazoline

No.	**Symbol**	**Definition**[b]
1	CH_3 ss	$(r_1 + r_2 + r_3)/\sqrt{3}$, $(r_4 + r_5 + r_6)/\sqrt{3}$), $(r_7 + r_8 + r_9)/\sqrt{3}$)
4-6	CH_3 ips	$(2r_1 + r_2 + r_3)/\sqrt{6}$, $(2r_4 + r_5 + r_6)/\sqrt{6}$, $(2r_7 + r_8 + r_9)/\sqrt{6}$
7-9	CH_3 ops	$(r_2 – r_3)/\sqrt{2}$, $(r_5 – r_6)/\sqrt{2}$, $(r_8 – r_9)/\sqrt{2}$
10	CH_2ss	$(\gamma_{10} + \gamma_{11}) / \sqrt{2}$
11	CH_2ass	$(\gamma_{10} – \gamma_{11}) / \sqrt{2}$
12-15	CC	S_{12}, S_{13}, S_{14}, S_{15})
16 – 17	CO	R_{16}, R_{17}
18-19	CN	T_{18}, T_{19}
20	R bend 1	π_{20}+a $(\pi_{21}+\pi_{22})$ +b $(\pi_{23}+\pi_{24})$
21	R bend 2	(a-b) $(\pi_{21}-\pi_{22})$ + (1-a) $(\pi_{23}+\pi_{24})$
22-24	CH_3sb	$(- \lambda_{25} -\lambda_{26} -\lambda_{27} + \sigma_{34} + \sigma_{35} + \sigma_{36})/\sqrt{6}$, $(- \lambda_{28} - \lambda_{29} - \lambda_{30} + \sigma_{37} + \sigma_{38} + \sigma_{39})/\sqrt{6}$, $(-\lambda_{31} - \lambda_{32} - \lambda_{33} + \sigma_{40} + \sigma_{41} + \sigma_{42})/\sqrt{6}$
25-27	CH_{3ipb}	$(-\sigma_{34} - \sigma_{35} - 2\sigma_{36})/\sqrt{6}$, $(-\sigma_{37} - \sigma_{38} - 2\sigma_{39}$ -)/$\sqrt{6}$, $(- \sigma_{40} - \sigma_{41} - 2\sigma_{42})/\sqrt{6}$
29-30	CH_{3opb}	$(\sigma_{34} - \sigma_{35})/\sqrt{6}$, $(\sigma_{37} - \sigma_{38})/\sqrt{6}$, $(\sigma_{40} - \sigma_{41})/\sqrt{6}$
31-33	CH_{3ibr}	$(2\lambda_{25} - \lambda_{26} - \lambda_{27})/\sqrt{6}$, $(2\lambda_{28} - \lambda_{29} - \lambda_{30})/\sqrt{6}$, $(2\lambda_{31} - \lambda_{32} - \lambda_{33})/\sqrt{6}$
34-36	CH_{3opr}	$(\lambda_{26} - \lambda_{27})/\sqrt{2}$, $(\lambda_{29} - \lambda_{30})/\sqrt{2}$, $(\lambda_{32} - \lambda_{33})/\sqrt{2}$
37	CH_{2scis}	$\beta_{43} + \beta_{45} + \beta_{44} + \beta_{46}$
38	CH_{2wag}	$\beta_{43} – \beta_{45} + \beta_{44} - \beta_{46}$
39	CH_{2twist}	$\beta_{43} – \beta_{45} - \beta_{44} + \beta_{46}$
40	CH_{2rock}	$\beta_{43} + \beta_{45} - \beta_{44} + \beta_{46}$
41	bcc	$(\theta_{47} - \theta_{48})/\sqrt{2}$
42	bcc	$(\xi_{49} - \xi_{50})/\sqrt{2}$
43	bcc	$(\varepsilon_{51} - \varepsilon_{52})/\sqrt{2}$
44-46	ωcc	ω_{53}, ω_{54}, ω_{55}
47	R torsion 1	$\tau_{58} + b(\tau_{56} + \tau_{60}) + a(\tau_{57} + \tau_{59})$
48	R torsion 2	(a-b) $(\tau_{59} + \tau_{57})$ + (1–a) $(\tau_{60} - \tau_{56})$
49-51	t CH_3	τ_{61} , τ_{62} , τ_{63}

[b] For numbering of atoms refer Fig.1.

Table 4. Vibrational assignment of fundamental observed frequencies and calculated frequencies using HF/6-311++G(d,p) and B3LYP/6-311++G(d,p) level (wave number cm^{-1}; IR intensities (km $mole^{-1}$); Raman intensity (normalised to 100); force constant (mdyne A^{-1})] and probable assignments

Symmetry Species C1	Observed fundamentals (cm^{-1})		Calculated frequencies (cm^{-1})										Assignment TED%
			HF/6-311++G(d,p)					B3LYP/6-311++G(d,p)					
	FT-IR	FT-Raman	Unscaled	Scaled	IR intensity	Raman intensity	Force constant	Unscaled	Scaled	IR intensity	Raman intensity	Force constant	
A′	2965(vs)		3332	2971	9.8115	33.1098	7.209	3170	2962	4.8826	33.6144	6.521	CH_3ss(98)
”		2960(vs)	3295	2966	46.3392	39.1188	7.114	3125	2963	38.0594	61.1987	6.340	CH_3ss(98)
”	2953(s)		3283	2957	59.7839	63.4226	6.998	3122	2955	13.3445	16.7520	6.334	CH_3ss(97)
”		2936(s)	3280	2946	13.9464	46.6723	6.982	3115	2941	8.2388	46.0550	6.292	CH_3ips(97)
”	2982		3276	2939	2.0172	7.9717	6.979	3108	2937	42.0062	64.2797	6.270	CH_3ips(98)
”		2903(s)	3260	2898	56.8540	66.0762	6.894	3107	2890	28.7723	32.3057	6.317	CH_3ips(97)
”	2894(s)		3255	2896	21.2378	14.2852	6.868	3105	2891	5.0322	21.9427	6.261	CH_3ops (87)
”	2872(w)		3251	2874	54.6711	83.4346	6.580	3060	2870	46.2392	104.5886	5.827	CH_3ops (87)
”		2866(ms)	3223	2870	16.3740	109.4946	6.356	3056	2862	11.4104	142.8474	5.712	CH_3ops (88)
”	2727(w)		3202	2736	35.0358	158.451	6.274	3038	2732	22.5039	157.9518	5.639	CH_2ss(89)
”	2713(vw)		3194	2719	30.8742	0.1354	6.245	3034	2718	26.3713	0.5107	5.617	CH_2 ass(82)
”	1781(w)		1925	1789	282.3933	48.6165	22.603	1738	1785	187.4901	57.7334	17.628	γ CN (82)
”	1739(w)		1678	1744	1.7325	11.1338	1.827	1526	1741	1.3225	13.2813	1.496	γ CN (82)
”	1689(vs)		1646	1695	7.5508	3.3658	1.686	1510	1691	11.3067	5.3759	1.413	γ CC (83)
”		1679(s)	1638	1679	2.6801	32.0207	1.682	1501	1675	5.0689	23.9954	1.407	γ CC (84)
”	1674(w)		1627	1675	2.1608	14.7860	1.637	1493	1670	2.2123	14.9135	1.375	γ CC (83)
”		1666(vw)	1621	1674	0.3656	18.6732	1.623	1483	1670	0.5676	14.8044	1.357	γ CC (84)
”	1490(s)		1617	1485	8.1144	42.4124	1.643	1483	1480	11.6863	48.3350	1.373	γ CO (83)
”	1465(s)		1616	1466	7.4447	23.4166	1.607	1482	1463	10.4368	16.2875	1.350	γ CO (84)
”		1458(w)	1573	1450	31.7202	2.6123	2.080	1426	1455	14.9958	2.7083	1.584	CH_3ipb(85)
”		1445(w)	1563	1445	12.0389	1.1824	1.867	1418	1450	20.2422	7.1396	1.592	CH_3ipb(84)
”	1436(w)		1549	1436	9.0017	0.0783	1.842	1404	1429	11.6024	0.5021	1.467	CH_3ipb(85)
”	1409(s)		1530	1426	7.5406	6.4310	2.029	1376	1418	12.0995	7.2570	1.636	CH_2 sciss(86)
”	1390(vs)		1435	1386	115.1156	11.7761	3.922	1295	1382	83.2393	11.1316	3.254	CH_3sb(85)
”		1384(s)	1395	1376	9.1799	3.9821	2.108	1267	1380	9.0533	4.3214	1.910	CH_3sb(84)
”	1378(w)		1354	1369	38.7022	8.8084	2.864	1221	1374	43.8818	10.0971	2.039	CH_3sb(85)
”	1369(ms)		1323	1362	33.3715	7.8739	2.555	1199	1350	18.6661	7.2762	2.211	CH_3obp(78)
”		1352(s)	1317	1360	0.0346	25.9428	1.442	1197	1355	0.2556	24.0360	1.153	CH_3opb(77)
”	1346(w)		1187	1337	44.2806	11.751	2.154	1067	1338	1.3786	0.3281	1.059	CH_3opb(78)
”	1276(vs)		1173	1267	1.2707	1.0352	1.313	1064	1268	13.2894	12.9269	1.382	CH_3ipr (77)
”	1201(vs)		1134	1241	2.2549	9.3131	1.044	1035	1223	1.5578	5.2812	0.869	CH_3ipr(78)
”		1179(s)	1130	1209	50.6941	5.2236	3.044	1016	1192	63.5541	3.3141	4.651	CH_3ipr(76)
”		1049(ms)	1068	1175	12.3338	21.7804	1.225	976	1156	11.8526	19.2612	1.054	CH_3 opr(66)
”	1038(s)		1056	1069	1.1419	0.0855	0.817	968	1060	0.9951	0.0547	0.688	CH_3 opr(65)
”	992(vs)		1042	1052	25.6761	22.7891	2.120	934	1013	22.7767	13.9351	1.988	CH_3 opr(65)
”	940(vs)		1009	965	0.7677	46.6598	1.010	930	960	0.2656	36.2607	0.867	R bend1(76)
”		926(ms)	979	956	19.4295	21.3625	1.331	884	940	20.2338	19.1371	1.117	R bend2(74)
”	918(w)		902	936	6.8861	48.4637	2.235	827	925	3.7407	41.5041	1.895	CH_2wag
”		885(ms)	715	932	5.6984	26.3881	1.321	665	901	3.5819	24.0095	1.1485	bcc (66)
”	874(vs)		701	913	14.7223	4.9006	1.142	637	895	7.7475	1.1051	1.010	bcc (65)
”		822(vs)	640	884	14.1513	0.4012	0.884	596	806	1.2670	84.9778	0.774	bcc (64)
”	811(s)		491	832	1.1769	4.8545	0.401	450	819	2.8554	5.6463	0.336	CH_2twist(69)
”	680(s)		470	824	1.4401	1.4038	0.3296	440	808	1.4003	2.8308	0.283	ω cc(55) bcc(22)
”		665(s)	362	674	0.5501	10.074	0.186	336	653	0.6521	14.7005	0.162	ω cc(54) bcc(21)
”	655(vs)		360	671	2.7506	8.0844	0.1658	332	644	2.4943	13.5715	0.143	ω cc(52) bcc(20)
”		629(vs)	326	638	2.0400	2.6695	0.106	301	619	2.5806	3.9160	0.109	tRtorsio 1(60)
”		597(w)	282	606	1.2928	0.0670	0.061	254	587	0.8102	0.0513	0.044	τR torsi 2(61)
”	463(ms)		259	472	0.0197	0.2865	0.042	229	456	0.0023	0.3505	0.0331	CH_2roc(67)bcc(20)
”		340(s)	184	319	3.2097	1.9429	0.045	172	331	3.2605	4.1663	0.041	τCH_3 (54)
”		300(w)	157	309	1.1967	3.4748	0.017	133	289	0.9501	5.5994	0.0118	τCH_3 (55)
”		180(w)	21	192	0.0030	12.1008	0.001	26	175	0.0309	19.4789	0.001	τCH_3 (54)

Abbreviations: ν – stretching; ss – symmetric stretching; ass – asymmetric stretching; b – bending; ω - out-of-plane bending; R – ring; trigd – trigonal deformation; symd – symmetric deformation; asymd – antisymmetric deformation; t – torsion; s – strong; vs – very strong; ms – medium strong; w – weak; vw – very weak.

Table 5. The thermodynamical parameters 2,4,4-trimetlyl-2-oxazoline along with the global minimum energy calculated at the HF/B3LYP methods and basis set

Parameter	Methods/Basis set	
	HF/6-311++G(d,p)	B3LYP/6-311++G(d,p)
Total energy (thermal), E_{total} (k cal mol^{-1})	112.366	109.394
Heat capacity cv. (k cal mol^{-1})	0.03214	0.010939
Entropy.S (k cal $mol^{-1}K^{-1}$)	0.09241	0.09038
Total		
Translational	0.04156	0.04008
Rotantional	0.02853	0.028115
Vibrational	0.02341	0.022187

Vibrational energy, E $_{vib}$ (k cal mol^{-1})	61.723	57.507
Zero point vibrational energy, (k cal mol^{-1})	109.792	103.9442
Rational constants(GHz)		
A	3.6120	3.6296
B	1.5921	1.6098
C	1.4713	1.4627
Dipole moment (Debye)		
μ_x	0.4186	0.4276
μ_s	0.9432	1.0641
μ_z	-0.0021	0.0010
μtotal	1.3412	1.1417

Table 6. The charge distribution calculated by the Mulliken method for 2,4,4-trimetlyl-2-oxazoline

Atoms	**Method / Basis set**	
	HF/6-311++G(d,p)	**B3LYP/6-311++(d,p)**
O1	-.8108	-0.2181
C2	0.8622	0.3614
N3	-0.8071	-0.1815
C4	0.3039	-0.2675
C5	0.3433	-0.2836
C6	-0.0025	-0.8510
H7	0.0296	0.2316
H8	0.02964	0.2241
H9	0.037701	0.2410
C10	0.03703	-0.5172
H11	-0.02186	0.2016
H12	0.01509	0.2110
H13	0.0064	0.1953
C14	0.03707	-0.3791
H15	0.01509	0.1950
H16	-0.0064	0.2103
H17	-0.0148	0.2007
H18	-0.01481	0.2183
H19	-0.01502	0.2041

Table 7. Second order perturbation theory analysis of Fock matrix in NBO basis for 2,4,4-trimetlyl-2-oxazoline using B3LYP/6-311++G(d,p) level calculation

Donor(i)	**Type**	**Acceptor(j)**	**Type**	**E$^{(2)a}$ (kJ mol^{-1})**	**ε_j–ε_i^{b} (a.u.)**	**F(i,j)^c (a.u)**
O1 – C2	σ	C2 - C6	σ*	7.28	1.60	0.077
		C2 – N3	σ*	2.24	1.65	0.055
C2 – N3	π	C4 – C10	σ*	2.05	1.57	0.051
		C4 – C14	σ*	8.19	0.97	0.080
N3 - C4	σ	O1 – C5	σ*	4.55	1.36	0.070
		C2 – C6	σ*	5.02	1.49	0.077
C4 – C5	σ	C4 – C10	σ*	2.30	1.55	0.54
		C4 – C14	σ*	1.77	1.55	0.047
		C14 – H17	σ*	2.00	1.50	0.049
C6-H7	σ	C2 – N3	π*	8.16	0.84	0.078
C10-H11	σ	N3 - C4	σ*	4.77	1.30	0.071
C14-H16	σ	N3 - C4	σ*	5.97	1.30	0.079
L1(O1)	σ	C2 - N3	π*	9.15	1.38	0.100

[a] E$^{(2)}$ means Energy of hyper conjugative interaction

[b] ε_i-ε_j means Energy difference between donnor and acceptor i and j NBO orbitals.

[c] F(i,j) is the Fock matrix element between i and j NBO orbitals.

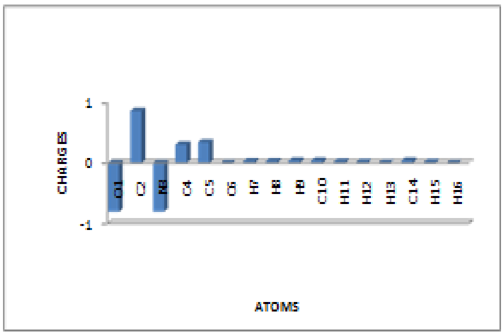

HF

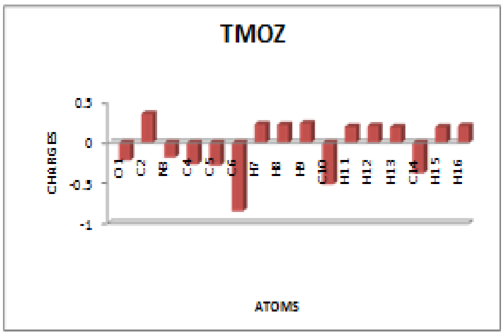

B3LYP

Fig 4. Plot of Mulliken's charges obtained by HF, B3LYP/6-311++G(d,p) method

In this theory the electron delocalization is signified as the interaction between occupied molecular natural orbitals in one fragment of the molecule with particular unoccupied molecular orbitals in another fragment of the molecule. According to this theory the total electron density is characterized by localized orbitals, which allows the representation of molecules in terms of localized Lewis-type structures. The electron delocalizations, which can be considered as an intramolecular donor–acceptor interaction of localized bonds or lone pairs with antibonding orbitals, result in the departure from the hypothetical idealized Lewis structures due to conjugation. Amidst such conjugative interactions the electron density is transferred from occupied orbitals to unoccupied orbitals resulting in a loss of occupancies of the localized bonds and lone pairs, and in larger occupancies of the antibonding orbitals. Second-order perturbation energies (referred to as $E^{(2)}$) that are calculated by the NBO scheme reflect the strength of donor–acceptor (or bond–antibond) hyperconjugative interactions between NBOs and estimate the energetic importance of these interactions [44].

The natural bond orbital (NBO) analysis provides a description of the structure of a conformer by a set of localized bond, antibonds and Rydberg extravalence orbitals. Stabilizing interactions between filled and unoccupied orbitals and destabilizing interactions between filled orbitals can also be obtained from this analysis [41,45-47]. Therefore, NBO theory is a valuable complement to the energetic and structural data presented above. DFT level computation is used to investigate the various second order interaction between the filled orbitals of one subsystem and vacant orbitals of another subsystem, which is a measure of the delocalization or hyperconjugation [48]. The hyperconjugative interaction energy was deduced from the second-order perturbation approach as:

$$E^{(2)} = -n_\sigma \frac{\langle \sigma | F | \sigma \rangle^2}{\sum \sigma^* - \sum \sigma} = -n_\sigma \frac{F_{ij}^2}{E}$$

Where $<\sigma|F|\sigma>^2$ or F_{ij}^2 is the Fock matrix element between i and j NBO orbitals, ε_σ and ε_σ^* are the energies of σ and σ^* NBO's, and n_σ is the population of the donor σ orbital.

Also, the NBO analysis is an efficient method for investigating charge transfer (CT) or hyperconjugative interaction in molecular systems. Some electron donor orbital, acceptor orbital and the interacting stabilization energies resulting from the second-order micro disturbance theory have been reported [49]. The larger the $E^{(2)}$ values, the more intensive is the interaction between electron donors and electron acceptors. The second-order perturbation theory analysis of Fock matrix in the NBO basis of the molecule shows strong intramolecular hyperconjugative interactions, which are presented Table 7.

The most important interaction (n-σ*) energies, related to the resonance in the molecules, are electron donation from the LP(1)O atom of the electron donating groups to the anti-bonding acceptor π*(C2–N3) leading to stabilization of 9.15 kCal/mol). The electron density of conjugated bond of aromatic ring (~1.8e) clearly demonstrates strong delocalization. These interactions are observed as an increase in ED in C–C anti-bonding orbital that weaken their respective bonds [50-52].

A very strong interaction energies has been observed between the σ (C2-N3) → σ* (C4-C14) and σ (O1-C2) → σ* (C2-C6) are 8.19 and 7.28 kCal/mol. respectively, clearly demonstrate the intramolecular hyperconjugative interactions, between O-C-CH3 and N-C-CH3 group is strong in the ground state for TMOZ These change transfer interactions of TMOZ are responsible for pharmaceutical and biological properties. Hence, the TMOZ structures are stabilized by these orbital interactions.

Homo – Lumo Analysis

Many organic molecules that containing conjugated π electrons are characterized hyperpolarizabilities and were analyzed by means of vibrational spectroscopy [53, 54]. In most cases, even in the absence of inversion symmetry, the strongest bands in the Raman spectrum are weak in the IR spectrum and vice versa. But the intra-molecular charge transfer from the donor to acceptor group through a single–double bond conjugated path can induce large variations of both the molecular dipole moment and the molecular polarizability, making IR and Raman activity strong at the same time. The experimental spectroscopic behavior described above is well accounted for by *ab initio* calculations in π conjugated system that predict exceptionally large FT-Raman and FT-IR intensities for the same normal modes. As observed in the title molecules the bands observed in FT-IR and FT-Raman Spectra show that the relative intensities in IR and Raman spectra are comparable resulting from the electron cloud movement through π conjugated frame work from electron donor to electron acceptor groups. The analysis of the wave function indicates that the electron absorption corresponds to the transit from the ground to the first excited state and is mainly described by one electron excitation from the highest occupied molecular orbital (HOMO) to the lowest unoccupied molecular orbital (LUMO). The LUMO, of π nature (*ie*. benzene ring) is molecular delocalized over chloro ethyl and one of the two chlorine atoms, consequently the HOMO → LUMO transition implies an electron density transfer to benzene ring of π-conjugated system from chloro ethyl and one of the two chlorine atoms. The atomic orbital compositions of the frontier molecular orbitals of TMOZ are sketched in Fig. 5.

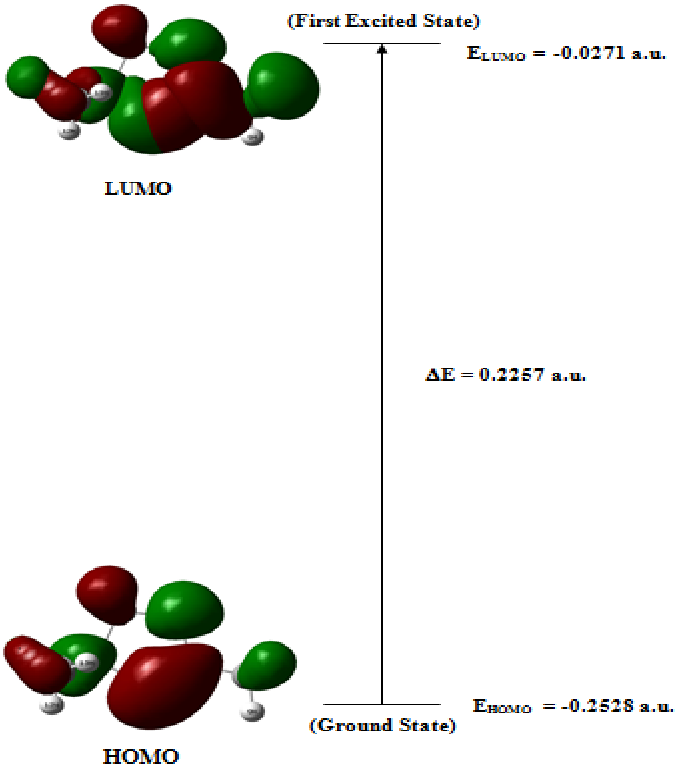

Fig 5. The atomic orbital compositions of frontier molecular orbital for 2,4,4,-trimethyl-2-oxazoline

The HOMO-LUMO energy gap of TMOZ calculated at the DFT 6-311++G (d,p) level as shown below, reveals that the energy gap reflects the chemical activity of the molecule.

LUMO as an electron acceptor represents the ability to obtain an electron; HOMO represents the ability to donoate an electron.

For TMOZ HOMO energy = –0.2528 a.u.
LUMO energy = –0.0271 a.u.
HOMO-LUMO energy gap = 0.2257 a.u.

Moreover, the lower value in the HOMO and LUMO energy gap explains the eventual charge transfer interactions taking place within the molecule [55-57].

Molecular Electrostatic Potential (MEP)

3D plots of molecular electrostatic potential contour map of TMOZ is shown in Fig. 6

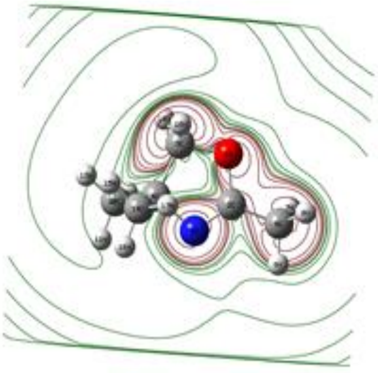

Fig 6. The contour map of electrostatic potential of 2,4,4-trimethyl-2-oxazoline

The MEP which is a plot of electrostatic potential mapped onto the constant electron density surface. The MEP is a useful property to study reactivity given than an approaching electrophile will be attracted to negative. In the majority of the MEPs, while the maximum negative region which preferred site for electrophilic attack indications as red color, the maximum positive region which preferred site for nucleophilic attack symptoms as blue color. The importance of MEP lies in the fact that it simultaneously displays molecular size, shape as well as positive, negative and neutral electrostatic potential regions in terms of color grading (Fig. 6) and is very useful in research of molecular structure with its physiochemical property relationship [58,59]. The resulting surface simultaneously displays molecular size and shape and electrostatic potential value.

Conclusion

DFT and *ab initio* calculations have been carried out on the structure and vibrational spectra of 2,4,4-trimethyl-2-oxazoline. Comparison between the calculated and experimental structural parameters indicates that B3LYP results are in good agreement with experimental values. Vibrational frequencies calculated by B3LYP/6-311++G (d,p) method agree well with experimental results. The assignments made at higher level of theory with higher basis set with only reasonable deviations from the experimental values, seem to be correct. The various properties of TMOZ are discussed by studying non-linear optical effects, thermodynamic properties and Mulliken atomic charges. HOMO and LUMO energy gaps explain the eventual charge transfer interactions taking place within the molecule. The NBO analysis reveals the reasons for hyperconjugative interaction, ICT (Intra-molecular charge transfer) and stabilization of molecule.

References

[1] P.L. Polavarapu, *J. Phys. Chem.* 94 (1990) 8106-8112.

[2] G. Keresztury, *Raman Spectroscopy Theory, in: J. M. Chalmers, P.R. Griffiths (eds). Handbook of vibrational spectroscopy,* Vol.1, John Wiley & sons Ltd., 2002, P. 71.

[3] G. Keresztury, S. Holly, J. Varga, G.Besenyci, A.Y. Wang, J.R. Durig, *Spectrochim. Acta Part A* 49 (1993) 2007-2026.

[4] M.J.Frisch, J.A.Pople, J.S.Binkley, *Journal of Chemical Physics,* 80 (1984) 3265.

[5] T.Clark, J.Chandrasekhar, G.W. Spitznagel, P.V.R. Schleyer, *Journal of Computational Chemistry* (1983) 294.

[6] T. Sundius., *Vibr. Spectrosc.* 29(2002) 89-95.

7] V. Arjunan, R.Santhanam, T.Ravi, H, Rosi, S. Mohan *Spectrochim. Acta Part A* 116 (2013) 182-196.

[8] K. Rastogi, M.A. Palafox, R.P. Tanwar, L. Mittal, Spectrochimica Acta A 58 (2002) 1989.

[9] M. Dien, Introduction to Modern Vibrational Spectroscopy, Wiley, New York,1993.

[10] P.B. Nagabalasubramanian, S. Periandy, S. Mohan, Spectrochimica Acta A 74 (2009) 277-280.

[11] J.H.S. Green, D.J. Harison, W. Kynoston, Spectrochimica Acta A 27 (1971) 807-815.

[12] K. Bahgat, N. Jasem, Talaat El-Emary, J. Serb. Chem. Soc. 74 (2009) 555.

[13] D.N. Sathyanarayana, Vibrational Spectroscopy - Theory and Applications, second ed., New Age International (P) Limited Publishers, New Delhi, 2004.

[14] M.Arivazhagan, R.Kavitha,. *Journal of Molecular Structure* 1011 (2012) 111–120.

[15] V.R. Dani, Organic Spectroscopy, Tata–McGraw Hill Publishing Company, New Delhi, 1995, p. 139.

[16] V. Krishnakumar, R. Mathammal, S. Muthunatesan, Spectrochimica Acta A 70 (2008) 210-216.

[17] R. John Xavier, E.Gobinath, Spectrochimica Acta A 91 (2012) 248-255.

[18] G. Shakila, S. Periandy, S. Ramalingam, Spectrochimica Acta A 86 (2012) 449-455.

[19] N.B. Colthup, L.H. Daly, S.E. Wiberley, Introduction to Infrared and Raman Spectroscopy, Third ed., Academic Press, Boston New York, MA 1990.

[20] M. Arivazhagan, R. Kavitha, J. Mol. 1011(2012) 111-120.

[21] B. Smith, Infrared spectra Interpretation, A systematic Approach, CRC press, Washington, DC 1999.

[22] M. Arivazhagan, D.Anitha Rexalin, J.Geethapriya, Spectrochimica Acta A 113 (2013) 236-249.

[23] N. Sundaraganesan, S. Ayyappan, H. Umamaheshwari, B. Dominic Joshua, Spectrochimica Acta 66 A (2007) 17-27.

[24] A. Kovacs, G. Keresztury, V. Izvekov, Chem. Phys. 253 (2000) 193-204.

[25] V. Krishnakumar, V. Balachandran, Spectrochimica Acta 16 A (2005) 1001-1006.

[26] S. Subash Chandrabose, H.Saleem, , Y.Erdogdu, O.Dereli, V.Thanikachalam, J. Jayabharathi, Spectrochimica Acta Part A, 86 (2012) 231-341.

[27] G. Litivinow, Proceedings of the XII International conference on Raman Spectroscopy, wurzburg, Germany, 1992.

[28] S.J. Singh, S.M. Pandey, Indian Journal of Pure and Applied Physics,12 (1974) 300-304.

[29] K. Furie, V. Mohacek, M. Bonifacic, I. Stefanic, Journal of Molecular Structure, 39 (1992) 262.

[30] G. Lau, H. Wang, Spectrochimica Acta 46 (1990) 1211.

[31] M. Mills, Spectrochimica Acta Part A, 19 (1963) 1585-1594.

[32] N. Sundaraganesan, B. Anand, C. Meganathan, B. Dominic Joshua, H. Saleem, Spectrochimica Acta A 69 (2008) 198-204.

[33] C.R. Zhang, H.S. Chen, G.H. Wang, *Chem. Res. Chin. U* 20 (2004) 640–646.

[34] Y. Sun, X. Chen, L. Sun, X. Guo, W. Lu, *Chem. Phys. Lett.* 381 (2003) 397–403.

[35] O. Christiansen, J. Gauss, J.F. Stanton, *Chem. Phys. Lett.* 305 (1999) 147–155.

[36] Z.S. Wang, Y.Y. Huang, C.H. Huang, J. Zheng, H.M. Cheng, S.J. Tian, *Synth. Met.*14 (2000) 201–207.

[37] T. Karakurt *et al. Journal of Molecular Structure* 991 (2011) 186–201.

[38] D.A.Kleinman, Phys. Rev. 126 (1962) 1977.

[39] M. Arivazhagan, R.Gayathri, Spectrochimica Acta Part A, 116 (2013) 170- 182.

[40] R.S. Mulliken, *J. Chem. Phys.* 23 (1955) 1833–1840.

[41] F. Weinhold, in: P.v.R. Schleyer, N.L. Allinger, T. Clark, J. Gasteiger, P.A. Kollman, H.F. Shaefer III, P.R. Schreiner (Eds.), *Encyclopedia of Computational Chemistry, vol. 3*, John Wiley & Sons, Chichester, UK, (1998) p. 1792.

[42] A.E. Reed, L.A. Curtiss, F. Weinhold, *Chem. Rev.* 88 (1988) 899-926.

[43] B.F. King, F. Weinhold, *J. Chem. Phys.* 103 (1995) 333-347.

[44] M. Dakkouri, V. Typke, *Journal of Molecular Structure* 978 (2010) 48–60.

[45] J.P. Foster, F. Weinhold, *J. Am. Chem. Soc.* 102 (1980) 7211-7218.

[46] F. Weinhold, C.R. Landis, *Valency and Bonding: A Natural Bond Orbital Donor–Acceptor Perspective*, Cambridge University Press, New York, 2005.

[47] H.W. Thomson, P. Torkington, *J. Chem. Soc.* (1945) 640-645.

[48] E.D. Glendening, J.K. Badenhoop, A.E. Reed, J.E. Carpenter, J.A. Bohmann, C.M. Morales, F. Weinhold, *NBO 5.0, Theoretical Chemistry Institute, University of Wisconsin*, Madison, 2001.

[49] C. James, A. Amal Raj, O.F. Nielson, V.S. Jayakumar, I. Hubert Joe, *Spectrochim. Acta*. 70A (2008) 1208-1216.

[50] B.Smith, *Infrared Spectral Interpretation, A. Systematic approach*, CRC press, Washington, DC, 1999.

[51] M. Arivazhagan, S.Jeyavijayan, J.Geethapriya, Spectrochimica Acta Part A, 104 (2013) 14-25.

[52] V.Thanikachalam, V. Periyanayagasamy, J. Jayabharathi, G. Manikandan, H.Saleem, S. Subash Chandrabose, Y.Erdogdu, Spectrochimica Acta Part A, 87 (2012) 86-95.

[53] T. Vijayakumar, I. Hubert Joe, C.P.R. Nair, V.S. Jayakumar, *Chem. Phys.* 343 (2008) 83-99.

[54] M.A. Palafox, *Int. J. Quant. Chem.* 77 (2000) 661-684.

[55] M. Arivazhagan, R. Meenakshi, S.Prabhakaran, Spectrochimica Acta Part A, 102 (2013) 59-65.

[56] R. John Xavier, E.Gobinath, Spectrochimica Acta A 86 (2012) 235-242.

[57] N.Sundaraganesan, G. Mariappan, S. Manoharan, Spectrochimica Acta A 87 (2012) 67-78.

[58] M. Arivazhagan, P. Muniappan, R. Meenakshi, G. Rajavelu, Spectrochimica Acta Part A, 105 (2013) 497-508

[59] C. Sridevi, G. Shanthi, G.Velraj, Spectrochimica Acta A 89 (2012) 46-56.